DOI: 10.47743/achi-2025-1-0007 ACTA CHEMICA IASI, **33_1**, 123–142 (2025)

SODIUM HYDROXIDE-TREATED BETA-CYCLODEXTRIN HYDROCHAR FOR MALACHITE GREEN REMOVAL

Siti Farah Inani Zulkifly[a,b], Fadina Amran [a,b], and Muhammad Abbas Ahmad Zaini[a,b]*

[a]*Centre of Lipids Engineering & Applied Research (CLEAR), Ibnu-Sina Institute for Scientific & Industrial Research (ISI-SIR), Universiti Teknologi Malaysia, 81310 UTM Johor Bahru, Johor, Malaysia*

[b]*Faculty of Chemical & Energy Engineering, Universiti Teknologi Malaysia, 81310 UTM Johor Bahru, Johor, Malaysia*

Abstract: In this work, beta cyclodextrin hydrochar was treated using sodium hydroxide for malachite green removal. The adsorbents were characterized for surface functionalities, thermal decomposition and morphology. The functionalized hydrochar exhibits the adsorption-precipitation mechanisms with maximum capacity of 76.9 mg/g, prior to surface neutralization by dye solution that results in the decrease of capacity. The equilibrium curve for adsorption-precipitation regime obeys Freundlich model, while the kinetic follows pseudo-first order model, both suggesting the physical adsorption process. From the thermodynamic perspective, the process is exothermic and spontaneous.

***Keywords*:** Adsorption, beta-cyclodextrin hydrochar, malachite green, sodium hydroxide treatment

Introduction

Water pollution usually results from the industrial discharge and indiscriminate release of commercial, domestic and agricultural effluents

* Muhammad Abbas Ahmad Zaini, *e-mail:* abbas@cheme.utm.my

into streams. The contamination leads to a decrease in water quality and brings a threat to the environment and public health.[1] The prevalent health concerns include skin disorders, diarrhoea, stomach ulcers and respiratory infections.[2] Water pollutants encompass chemicals,[3] pathogens,[4] excessive nutrients,[5] trash and debris[6] and radioactive material,[7] depending on the point-source of the effluent. Wastewater treatment is critical in ensuring the effluent is safe prior to discharge to the environment.[8] Among others, adsorption is a preferred method because of its simple and straightforward operation, low-cost and efficient in removing various contaminants from water.[9]

Dyes are usually used in textiles, food, paint and paper industries. Even in small quantities, their presence in effluent is vivid and undesirable. Because of the complex aromatic structure, dyes are difficult to breakdown and hence tend to stay in the water environment.[10] Malachite green is a commonly used cationic dye in textile and related industries that is persistent in the environment and harmful to the aquatic and terrestrial creatures, particularly freshwater fish.[11]

To date, beta-cyclodextrin (β-CD) has gained considerable reputation in water pollution abatement due to its unique hydrophilic-hydrophobic molecular cavity able to entrap various types of water pollutants. This property has been capitalized, not only in separation and adsorption, but also for drug-controlled release.[12] However, the solubility characteristic of β-CD in water remains a challenge for its direct use in wastewater treatment. Therefore, attempt has been made in this work to produce β-CD hydrochar followed by sodium hydroxide treatment for malachite green removal. The adsorbent was characterized and the removal of dye was analyzed from the viewpoints of isotherm and kinetics. Also, the

governing mechanisms were discussed to shed insight into practical wastewater treatment process.

Experimental

Materials

Beta-cyclodextrin (β-CD) was purchased from Jiangsu Ogo Biotech Co. Ltd., China. Malachite green was supplied by HmBG Chemicals (Hamburg, Germany). All chemicals and reagents are of analytical grade.

Preparation of adsorbent

The β-CD was insolubilized by hydrothermal carbonization in a Teflon autoclave at 180 °C for 24 h. The resultant hydrochar (designated as BCD-h) was further impregnated using sodium hydroxide at ratio of 2:1 (w/w, NaOH pellet-to-BCD-h) prior to pyrolysis at 550 °C for 1.5 h (heating rate=25 °C/min). The NaOH-treated β-CD hydrochar (labelled as BCD-h+NaOH) was rinsed with distilled water and oven-dried prior to use.

Characterization of materials

The FTIR spectrometer (model IRTracer-100) was used to identify surface functional groups in BCD-h and BCD-h + NaOH. The spectra were recorded in the range of 4000–400 cm^{-1}. The thermal degradation profiles of BCD-h were obtained using a thermogravimetric analyzer (TGA) under N_2 flow at a heating rate of 10 °C/min from room temperature to 900 °C. The weight loss pattern provides insight into the changes in composition and thermal stability. The surface morphology of BCD-h and BCD-h + NaOH was captured using a Hitachi TM 3000 field emission scanning electron microscope.

Batch adsorption studies

30 mg of adsorbent was added into several flasks containing 30 mL dye solution of varying concentrations ranging from 5 mg/L to 500 mg/L. The mixture was allowed to equilibrate for 5 days, and the residual concentration was measured using a visible spectrophotometer. The adsorption behavior at equilibrium was analyzed using Langmuir and Freundlich models. The Langmuir model is expressed as,

$$Q_e = \frac{Q_m b C_e}{1 + bC_e} \quad (1)$$

where Q_e (mg/g) represents the malachite green capacity per gram of adsorbent and C_e (mg/L) is the equilibrium concentration of dye in the solution. The constants, Q_m (mg/g) and b (L/mg) represent the maximum adsorption capacity and Langmuir binding affinity, respectively.[13] The Freundlich model is expressed as,

$$Q_e = K_f C_e^{\frac{1}{n}} \quad (2)$$

where K_f (mg/g)(L/mg)$^{1/n}$ is the Freundlich capacity and n is an index to show the effectiveness of the process.[14]

The rate of malachite green adsorption was evaluated at concentrations of 10 mg/L and 25 mg/L. 30 mg of BCD-h+NaOH was added into 30 mL of dye solution and measuring of residual concentration was performed at pre-set time intervals until the equilibrium is attained. The kinetics data were fitted into pseudo-first order and pseudo-second order models. The pseudo-first order equation is given by:

$$Q_t = Q_e[1 - \exp(-k_1 t)] \quad (3)$$

the time and k_1 (min^{-1}) is the pseudo-first order rate constant. The pseudo-second order equation is given as,

$$Q_t = \frac{k_2 Q_e^{\,2} t}{1 + k_2 Q_e t} \tag{4}$$

where k_2 (g/mg.min) is the pseudo-second order rate constant.[15]

A fixed dye concentration of 100 mg/L was employed to assess the effect of temperature on malachite green removal. The experiment was conducted at varying solution temperatures: 40, 50 and 60 °C, achieved by adjusting the water bath temperature. The mixture was allowed to stand for 5 days, then the change in concentration was measured. The thermodynamic parameters were established from the expression of Gibbs free energy,

$$\Delta G^\circ = \Delta H^\circ - T\Delta S^\circ \tag{5}$$

where $\Delta G°$ (kJ/mol), $\Delta H°$ (kJ/mol) and $\Delta S°$ (kJ/mol.K) are the change in Gibbs free energy, enthalpy and entropy, respectively, and T (K) is the solution temperature. The van't Hoff plot can be derived from Equation (5), and is often used to study the temperature dependence of adsorption process.[16] It can be expressed as,

$$\ln K_d = \frac{\Delta S^\circ}{R} - \frac{\Delta H^\circ}{RT} \tag{6}$$

where K_d is the equilibrium constant.

Results and Discussion

Characterization of adsorbents

Figure 1 shows the thermal degradation profiles of BCD-h. The material exhibits a steady decrease in mass as temperature increases. The initial weight loss of 4 % below 130 °C is likely attributed to the evaporation of adsorbed water from the adsorbent surface and cavity of

β-CD. Next, the degradation of free functional groups and the conversion of the polymer into monomers occurred between 230 °C and 300 °C.[17] The final weight loss of 15 % at a slower rate is attributed to the thermal decomposition of β-CD moieties.[18-20]

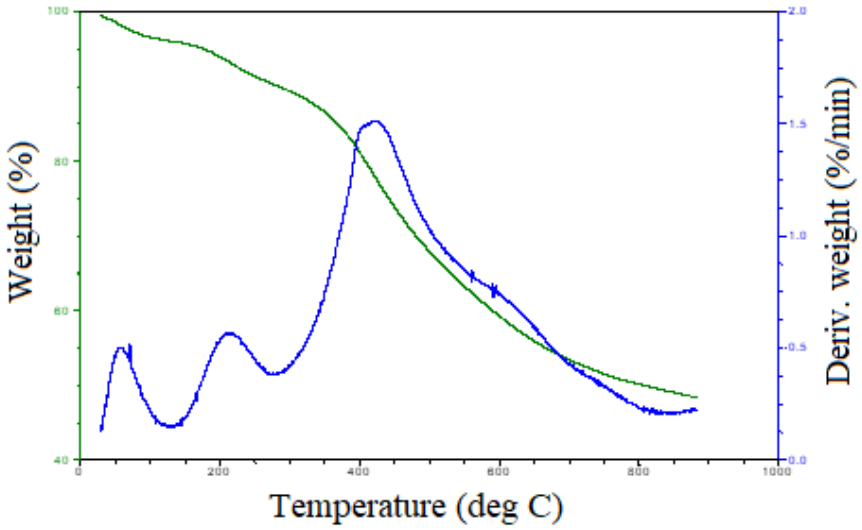

Figure 1. Thermal degradation profiles of BCD-h.

The degradation rate displays fluctuating trends, indicative of radical reactions at high temperature.[21] The adsorbent retained a 48.8 % of its mass at 800 °C, suggesting a thermal stability due to the highly crosslinked network.[22] This exceptional characteristic is advantageous for adsorbent regeneration in practical applications. A similar pattern for thermal degradation of β-CD-based adsorbents has been reported in literature.[17,20,22] However, chitosan/β-cyclodextrin composite retained only a 18.7 % mass, much lower compared to the one observed in this work.[17]

Figure 2 shows the FTIR spectra that offer a comprehensive insight into the surface functionalities of BCD-h and BCD-h+NaOH samples. The spectrum of BCD-h+NaOH becomes more simple (missing peaks) as compared to that of BCD-h upon treatment at high temperature. Notably,

the BCD-h spectrum contains peaks that correspond to several functional groups. The signals at 2913, 1691 and 1606 cm^{-1} are designated to asymmetric stretching vibration of CH_2 methylene groups, – OH stretching vibration and - CH bending vibration, respectively.[23] Additional peaks at 1287 and 1163 cm^{-1} are attributed to the bending vibration of hydroxide groups and the stretching vibration of C–OH. The C–OC stretching vibration and C–C bonds skeletal vibration could generate the peaks at 1020 and 862 cm^{-1}.[24] In contrast, the absence of prominent peaks in the BCD-h+NaOH spectrum is due to the release of heat-sensitive functional groups at high temperature and hydroxide ions shielding the BCD-h surface during activation. However, the stretching of hydroxyl and carboxyl groups is evident at 3738 cm^{-1}, while the peaks at 1412, 1159 and 876 cm^{-1} indicate –OH bending, C–OH stretching and C–C skeletal vibrations, respectively.

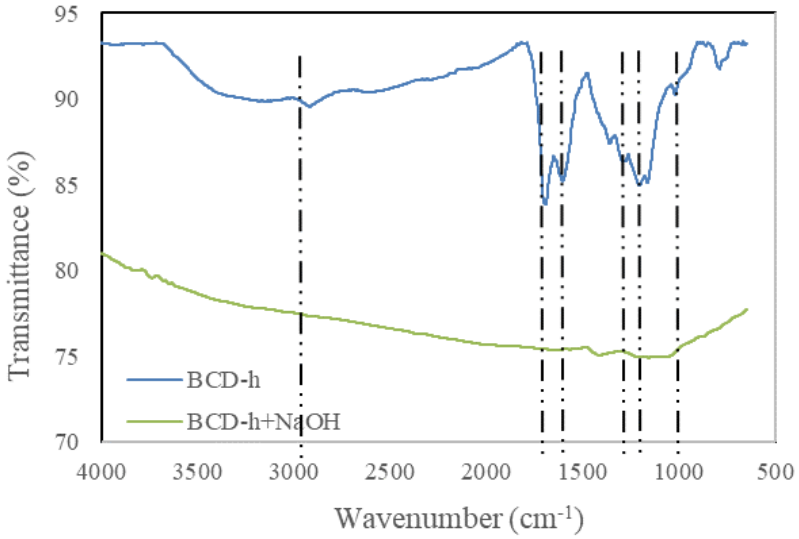

Figure 2. FTIR spectra for BCD-h and BCD-h+NaOH.

Figure 3 represents the morphology and physical structure of BCD-h and BCD-h+NaOH highlighted by SEM. The perfect spherical diameter of BCD-h considerably swollen and increased approximately fourfold after activation, suggesting the merging of neighboring particles.[25] The newly deformed microspheres are anticipated to play a crucial role in the removal of cationic dye during the adsorption process.

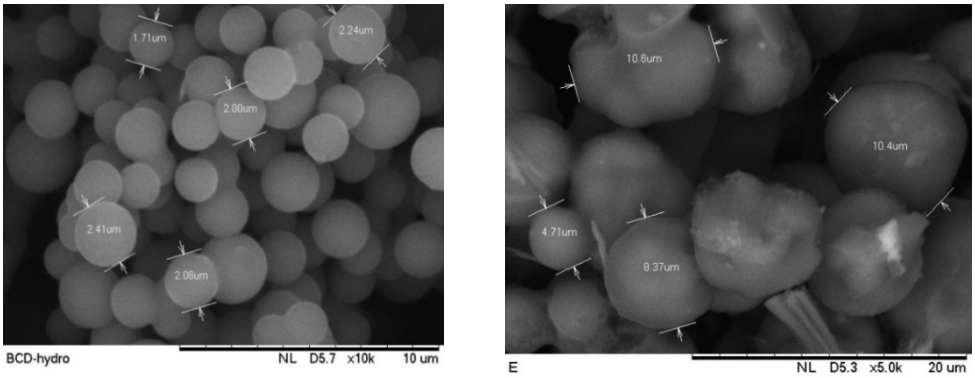

Figure 3. SEM images for BCD-h and BCD-h+NaOH.

Adsorption equilibrium

Figure 4 shows the adsorption equilibrium of malachite green by BCD-h+NaOH. The contact between the adsorbent and dye solution at initial concentrations of 5, 10, 20, 50, 100 and 200 mg/L results in the adsorption capacities of 1.67, 7.21, 15.5, 31.6, 50.5 and 76.9 mg/g, respectively. The removal capacity increased with increasing equilibrium concentration; the magnitude increased from 1.38 mg/g to 76.9 mg/g when the residual concentration increases from 0.015 mg/L to 63.3 mg/L. The dye concentration essentially provides the driving force to overcome mass transfer resistance to the adsorbent phase. Also, the increase in concentration enhances the interaction probabilities between the carbon surface and dye molecules.[26] An increase in dye concentration leads to an increase in the uptake of dye as long as the active sites are available to

accommodate the molecules. This is true to a point of surface saturation, at which the maximum capacity is reached. Similar trends were also reported for other malachite green adsorbents elsewhere.[11,27-29] BCD-h was also employed in the adsorption of malachite green. Nevertheless, the removal efficiency was so low, that this material was considered uninteresting to continue further subsequent adsorption analyses.

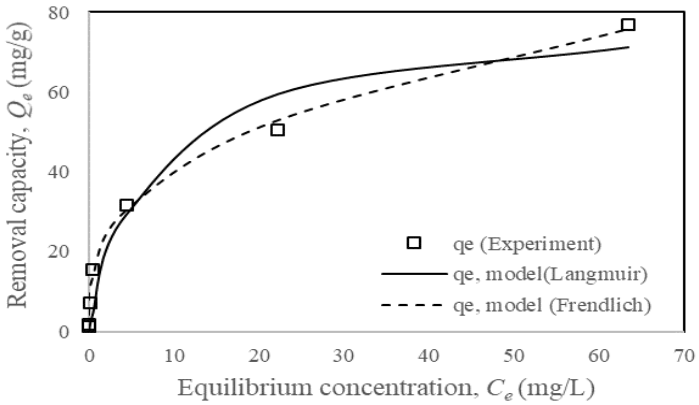

Figure 4. Equilibrium curve of malachite green adsorption by BCD-h+NaOH.

Table 2 shows the constants of Langmuir and Freundlich models. The values were computed by non-linear regression using *Solver* add-in of MS Excel.

Table 2. Isotherm constants for Langmuir and Freundlich models.

Isotherm model	Parameter	BCD-h+NaOH
Langmuir	Q_m (mg/g)	79.6
	b	0.130
	R^2	0.960
	SSE	311
Freundlich	K_f (mg/g)(L/mg)$^{1/n}$	18.4
	$1/n$	0.340
	R^2	0.990
	SSE	34.1

The equilibrium of malachite green adsorption by BCD-h+NaOH demonstrates a good fit to Freundlich model, evident from the higher regression coefficient (R^2) and smaller sum-of-squared error (SSE). It suggests that the adsorption process could be better described as physical adsorption where the adsorbate forms multiple layers on the adsorbent surface.

Effect of contact time

Figure 5 depicts the rate of malachite green adsorption onto BCD-h+NaOH at concentrations of 10 mg/L and 25 mg/L. The removal capacity increased with increasing retention time to a point where it reaches equilibrium. At equilibrium, the rate of adsorption is equal to the rate of desorption, and the magnitude of capacity tends to levelling off with time. The adsorption for C_o = 25 mg/L requires longer holding time of 200 min to attain equilibrium. At high concentration, the accumulation of dye molecules interferes the smooth diffusion towards the structure at highest energy sites.[30] Consequently, longer time will be required for adsorption because of inherent repulsion and resistance among dye molecules.

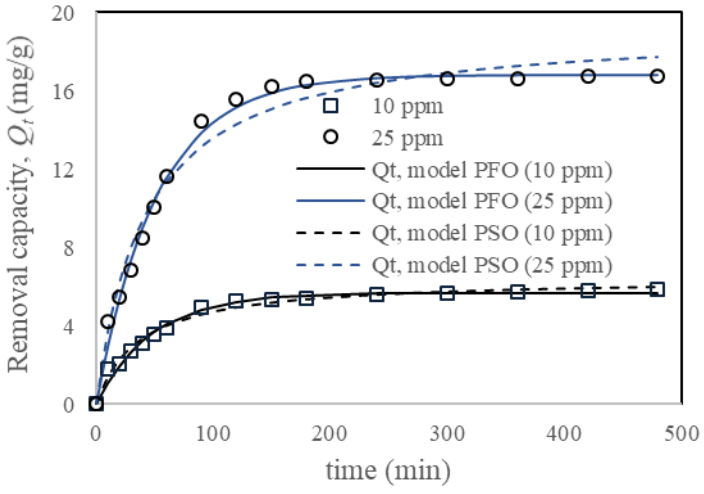

Figure 5. Rate of malachite green adsorption onto BCD-h+NaOH.

Table 3 summarizes the constants of the fore-mentioned kinetic models. It is apparent that BCD-h+NaOH obeys the pseudo-first order model for both concentrations studied. It is judged based on the values of R^2 and SSE, and closeness of the calcutated Q_e with the experimental ones. The applicability of this model implies the characteristics of physical adsorption. The rate constant, k_1 slightly decreased with concentration due to competition for active sites as concentration increases.

Table 3. Parameters for pseudo first order and pseudo second order models.

Kinetic model	Parameter	10 mg/L	25 mg/L
Pseudo-first order	Q_e (mg/g)	5.69	16.8
	k_1 (min^{-1})	0.0210	0.0190
	R^2	0.987	0.993
	SSE	0.713	3.21
Pseudo-second order	Q_e (mg/g)	6.43	19.3
	k_2 (g/mg.min)	$4.00x10^{-3}$	$1.00x10^{-3}$
	R^2	0.986	0.976
	SSE	0.679	10.8

Adsorption thermodynamics

Figure 6 shows the van't Hoff plot to determine the thermodynamic parameters, which are summarized in Table 4. The $\Delta H°$ is negative, indicating that the removal of malachite green is exothermic, whereby the adsorption decreased with temperature. The entropy measures the degree of disorder in the system; the negative $\Delta S°$ infers that the process is less favorable with increased orderliness or structural changes.[31] The formation of solid precipitate contributes to the structural rearrangement during the removal process, thus leading to negative $\Delta S°$.[32] Yet, the system $\Delta S°$ is

compensated by $\Delta H°$ for negative $\Delta G°$, which means that the overall process is thermodynamically spontaneous in nature.

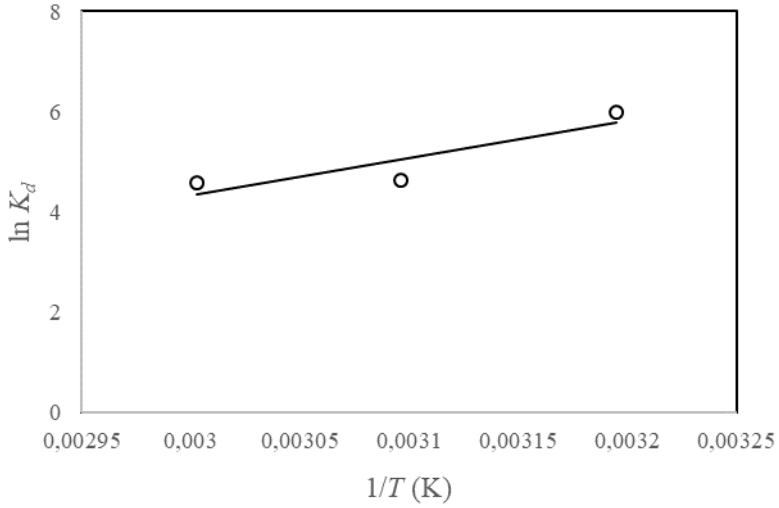

Figure 6. The van't Hoff plot.

Table 4. Thermodynamic parameters for malahite green adsorption onto BCD-h+NaOH.

T **(K)**	***K_d***	**Δ*G*° (kJ/mol)**	**Δ*H*° (kJ/mol)**	**Δ*S*° (kJ/mol.K)**
313	401	-15.1		
323	103	-13.6	-62.1	-0.150
333	97.0	-12.1		

Adsorption mechanisms

Figure 7 shows the equilibrium adsorption of malachite green spanning to C_o = 500 mg/L. Obviously, there is a fluctuating trend upon reaching a peak capacity at approximately 70 mg/g. It is suggested that the process undergone adsorption-precipitate mechanisms throughout the entire procedure.

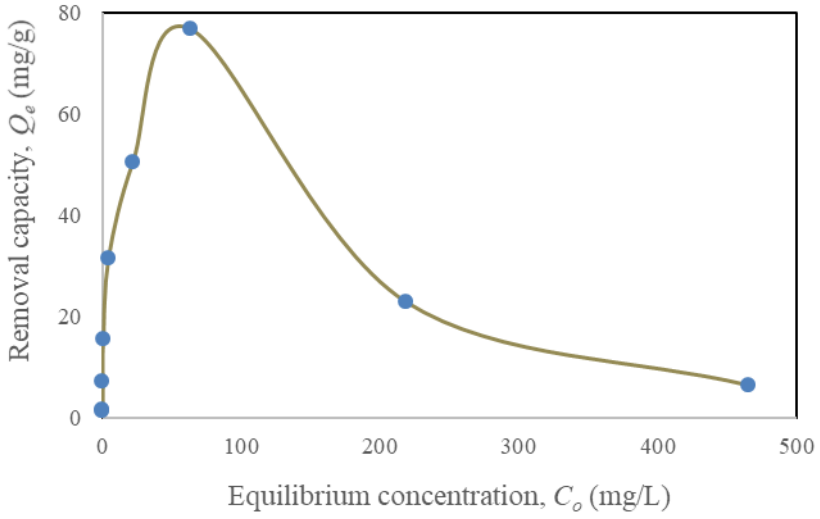

Figure 7. Equilibrium adsorption of malachite green at different concentrations.

The pyrolysis at 550 °C facilitates the disruption of ionic bonds of NaOH. Subsequently, the hydroxyl ions form a layer covering the surface of BCD-h+NaOH. The solution pH is notably elevated upon the addition of the adsorbent as the layer generated HO^- ions, especially for low malachite green concentration. In solution, the cationic malachite green (MG^+) interacts with HO^- to form solid precipitate MG–OH that becomes entrapped on the adsorbent surface.[33,34] However, the malachite green solution becomes more acidic at high concentration. Consequently, the solution endows high concentrations of MG^+ and H^+. At this point, the dissociated HO^- ions play a crucial role in neutralizing H^+ ions, so reducing the alkaline environment to propagate the precipitation. As a result, the capacity of malachite green through precipitation decreased with concentration and the removal is now shifted predominantly to adsorption (Figure 7). Figure 8 illustrates the mechanisms of malachite green removal.

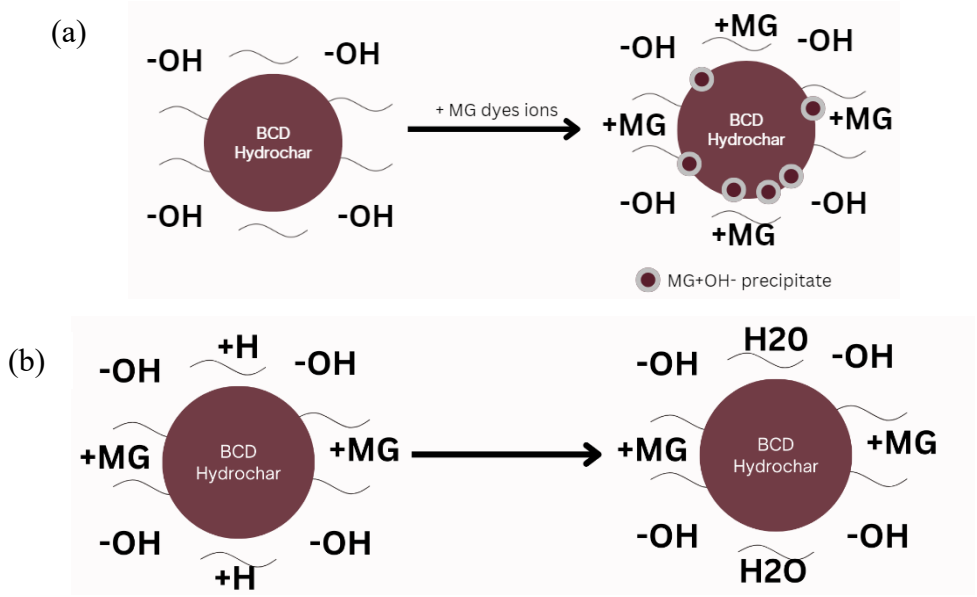

Figure 8. (a) Mechanisms of precipitation-adsorption process, and (b) neutralization of H^+ ions in the solution.

The primary interactions between β-CD and dye molecules include π-π interaction, dipole-dipole forces, van der Waals, hydrogen bonding, electrostatic interactions, host-guest interaction and hydrophobic effects.[35,36] The carboxyl and hydroxyl groups on the exterior engage in electrostatic interaction with the nitrogen of malachite green. Also, the electrostatic interaction is induced by both the readily adsorbed dye molecules and the neighboring dye molecules in the bulk solution.[37] Besides, malachite green has phenyl groups that offer host-guest supramolecular interactions with the hydrophobic cavity of β-CD.[38] Hydrogen bonding between the –OH groups of β-CD and the nitrogen of malachite green can also contribute to the adsorption process.

Conclusions

The sodium hydroxide-treated hydrochar (BCD-h+NaOH) was synthesized to study the removal of malachite green from water. The dye capacity reaches a maximum of 79.6 mg/g, and thereafter decreased with concentration revealing the adsorption-precipitation mechanisms. At this regime, the equilibrium fits well with Freundlich model, while the rate of adsorption could be described by pseudo-first order model, both suggesting the physical adsorption process with multiple layers of adsorbate on the carbon surface. The dye adsorption is thermodynamically spontaneous but the capacity decreased with temperature.

Acknowledgements

This work was fully funded by UTM FR No. 23H09.

References

1. Haseena, M.; Malik, M. F.; Javed, A.; Arshad, S.; Asif, N.; Zulfiqar, S.; Hanif, J. Water pollution and human health. *Environ. Risk Assess. Rem.* **2017**, *1*, 16 – 19. https://doi.org/10.4066/2529-8046.100020

2. Halder, J.; Islam, N. Water pollution and its impact on the human health. *J. Environ. Human.* **2015**, *2*, 36 – 46. https://doi.org/10.15764/EH.2015.01005

3. Chowdhary, P.; Raj, A.; Bharagava, R. N. Environmental pollution and health hazards from distillery wastewater and treatment approaches to combat the environmental threats: A Review. *Chemosphere* **2018**, *194*, 229 – 246. https://doi.org/10.1016/j.chemosphere.2017.11.163

4. Moges, F.; Endris, M.; Belyhun, Y.; Worku, W. Isolation and characterization of multiple drug resistance bacterial pathogens from waste water in hospital and non-hospital environments, Northwest Ethiopia. *BMC Res. Notes.* **2014**, *7*, 215. https://doi.org/10.1186/1756-0500-7-215

5. Akpor, O. B; Ohiobar, G. O.; Olaolu, T. D. Heavy metal pollutants in wastewater effluents: Sources, effects and remediation. *Adv. Biosci. Bioeng.* **2014**, *2*, 37. https://doi.org/10.11648/j.abb.20140204.11

6. Kuo, F. J.; Huang, H. W. Strategy for mitigation of Marine Debris: Analysis of sources and composition of marine debris in Northern Taiwan. *Mar. Pollut. Bull.* **2014**, *83*, 70 – 78. https://doi.org/10.1016/j.marpolbul.2014.04.019

7. Al-Taai, S. H. H. Water pollution its causes and effects. *IOP Conf. S.: Earth Environ. Sci.* **2021**, *790*, 012026. https://doi.org/10.1088/1755-1315/790/1/012026

8. Rout, P. R.; Zhang, T. C.; Bhunia, P.; Surampalli, R. Y. Treatment technologies for emerging contaminants in wastewater treatment plants: A Review. *Sci. Total Environ.* **2021**, *753*, 141990. https://doi.org/10.1016/j.scitotenv.2020.141990

9. Al Sharabati, M.; Abokwiek, R.; Al-Othman, A.; Tawalbeh, M.; Karaman, C.; Orooji, Y.; Karimi, F. Biodegradable polymers and their nano-composites for the removal of endocrine-disrupting chemicals (EDCS) from wastewater: A Review. *Environ. Res.* **2021**, *202*, 111694. https://doi.org/10.1016/j.envres.2021.111694

10. Crini, G. Studies on adsorption of dyes on beta-cyclodextrin polymer. *Bioresour. Technol.* **2003**, *90*, 193 – 198. https://doi.org/10.1016/S0960-8524(03)00111-1

11. Sartape, A. S.; Mandhare, A. M.; Jadhav, V. V.; Raut, P. D.; Anuse, M. A.; Kolekar, S. S. Removal of malachite green dye from aqueous solution with adsorption technique using *Limonia acidissima* (wood apple) shell as low cost adsorbent. *Arabian J. Chem.* **2017**, *10*, 3229 – 3238. https://doi.org/10.1016/j.arabjc.2013.12.019

12. Hu, J. Environmentally sensitive polymer gel and its application in the textiles field. In *Shape Memory Polymers and Textiles*; Woodhead Publishing Limited: United Kingdom, 2007, pp 252 – 278.

13. Fan, L.; Luo, C.; Sun, M.; Qiu, H.; Li, X. Synthesis of magnetic β-cyclodextrin–chitosan/graphene oxide as nanoadsorbent and its application in dye adsorption and removal. *Colloids Surf. B.* **2013**, *103*, 601 – 607. https://doi.org/10.1016/j.colsurfb.2012.11.023

14. Zhang, H.; Zhang, F.; Huang, Q. Highly effective removal of malachite green from aqueous solution by hydrochar derived from phycocyanin-extracted algal bloom residues through hydrothermal carbonization. *RSC Adv.* **2017**, *7*, 5790 – 5799. https://doi.org/10.1039/c6ra27782a

15. Simonin, J. P. On the comparison of pseudo-first order and pseudo-second order rate laws in the modeling of adsorption kinetics. *Chem. Eng. J.* **2016**, *300*, 254 – 263. https://doi.org/10.1016/j.cej.2016.04.079

16. Dauenhauer, P. J.; Abdelrahman, O. A. A universal descriptor for the entropy of adsorbed molecules in confined spaces. *ACS Cent. Sci.* **2018**, *4*, 1235 – 1243. https://doi.org/10.1021/acscentsci.8b00419

17. Jiang, Y.; Liu, B.; Xu, J.; Pan, K.; Hou, H.; Hu, J.; Yang, J. Cross-linked chitosan/β-cyclodextrin composite for selective removal of methyl orange: Adsorption performance and mechanism. *Carbohydr. Polym.* **2018**, *182*, 106 – 114. https://doi.org/10.1016/j.carbpol.2017.10.097

18. Shen, H.; Zhu, G.; Yu, W.; Wu, H.; Ji, H.; Shi, H.; She, Y.; Zheng, Y. Fast adsorption of p-nitrophenol from aqueous solution using β-cyclodextrin grafted silica gel. *Appl. Surf. Sci.* **2015**, *356*, 1155 – 1167. https://doi.org/10.1016/j.apsusc.2015.08.203

19. Zhao, F.; Repo, E.; Yin, D.; Meng, Y.; Jafari, S.; Sillanpaa, M. EDTA-crosslinked β-cyclodextrin: An environmentally friendly bifunctional adsorbent for simultaneous adsorption of metals and cationic dyes. *Environ. Sci. Technol.* **2015**, *49*, 10570 – 10580. https://doi.org/10.1021/acs.est.5b02227

20. Liu, N.; Wu, Y.; Sha, H. Characterization of EDTA-crosslinked β-cyclodextrin grafted onto Fe-Al hydroxides as an efficient adsorbent for methylene blue. *J. Colloid Interface Sci.* **2018**, *516*, 98 – 109. https://doi.org/10.1016/j.jcis.2018.01.056

21. Hao, F.; Guo, W.; Wang, A.; Leng, Y.; Li, H. Intensification of sonochemical degradation of ammonium perfluorooctanoate by persulfate oxidant. *Ultrason. Sonochem.* **2014***, 21*, 554 – 558. https://doi.org/10.1016/j.ultsonch.2013.09.016

22. Li, X.; Zhou, M.; Jia, J.; Ma, J.; Jia, Q. Design of a hyper-crosslinked β-cyclodextrin porous polymer for highly efficient removal toward bisphenol A from water. *Sep. Purif. Technol.* **2018**, *195*, 130 – 137. https://doi.org/10.1016/j.seppur.2017.12.007

23. Omar, N. H. M.; Zaini, M. A. A. Beta-cyclodextrin carbon microspheres by hydrothermal carbonization for malachite green adsorption. *Fullerenes, Nanotubes Carbon Nanostruct.* **2022**, *31*, 182 – 189. https://doi.org/10.1080/1536383X.2022.2136169

24. Nandiyanto, A. B.; Oktiani, R.; Ragadhita, R. How to read and interpret FTIR spectroscope of organic material. *Indonesian J. Sci. Technol.* **2019**, *4*, 97 – 118. https://doi.org/10.17509/ijost.v4i1.15806

25. Nguyen, V. L.; Le, A. K.; Ngo, V. T. H.; Nguyen, T. T.; Nguyen, T.; Tran, A. K. The influence of the functional groups and pore sizes on activated carbon for 4-chlorophenol adsorption by molecular simulation. *Chem. Eng. Trans.* **2023**, *106*, 913 – 918. https://doi.org/10.3303/CET23106153

26. Yagub, M. T.; Sen, T. K.; Ang, M. Removal of cationic dye methylene blue (MB) from aqueous solution by ground raw and base modified pine cone powder. *Environ. Earth. Sci.* **2014**, *71*, 1507 – 1519. https://doi.org/10.1007/s12665-013-2555-0

27. Abate, G. Y.; Alene, A. N.; Habte, A. T.; Getahun, D. M. Adsorptive removal of malachite green dye from aqueous solution onto activated carbon of *Catha edulis* stem as a low cost bio-adsorbent. *Environ. Syst. Res.* **2020**, *9*, 1 – 13. https://doi.org/10.1186/s40068-020-00191-4

28. Abewaa, M.; Mengistu, A.; Takele, T.; Fito, J.; Nkambule, T. Adsorptive removal of malachite green dye from aqueous solution using *Rumex*

abyssinicus derived activated carbon. *Sci. Rep.* **2023**, *13*, 14701. https://doi.org/10.1038/s41598-023-41957-x

29. Gurkan, E. H.; Coruh, S. Using waste foundry sand for the removal of malachite green dye from aqueous solutions-Kinetic and equilibrium studies. *Environ. Eng. Manag. J.* **2018**, *17*, 123 – 133. https://doi.org/10.30638/eemj.2018.014

30. Subramaniam, R.; Ponnusamy, S. K. Novel adsorbent from agricultural waste (cashew NUT shell) for methylene blue dye removal: Optimization by response surface methodology. *Water Resour. Ind.* **2015**, *11*, 64 – 70. https://doi.org/10.1016/j.wri.2015.07.002

31. Abodif, A. M.; Meng, L.; Ma, S.; Ahmed, A. S.; Belvett, N.; Wei, Z. Z.; Ning, D. Mechanisms and models of adsorption: TiO_2-supported biochar for removal of 3,4-dimethylaniline. *ACS Omega* **2020**, *5*, 13630 – 13640. https://doi.org/10.1021/acsomega.0c00619

32. Du, X.; Guang, W.; Cheng, Y.; Hou, Z.; Liu, Z.; Yin, H.; Huo, L.; Lei, R.; Shu, C. Thermodynamics analysis of the adsorption of CH_4 and CO_2 on montmorillonite. *Appl. Clay Sci.* **2020**, *192*, 105631. https://doi.org/10.1016/j.clay.2020.105631

33. Lee, Y. C.; Kim, E. J.; Yang, J. W.; Shin, H. J. Removal of malachite green by adsorption and precipitation using aminopropyl functionalized magnesium phyllosilicate. *J. Hazard. Mater.* **2011**, *192*, 62 – 70. https://doi.org/10.1016/j.jhazmat.2011.04.094

34. Latona, D. F.; Dada, A. O. Kinetics of Reaction between malachite green and hydroxyl ion in the presence of reducing sugars. *South Braz. J. Chem.* **2016**, *6*, 1021 – 1028. http://dx.doi.org/10.48141/SBJCHEM.v23.n23.2015.61_revista2015.pdf

35. Lee, J. U.; Lee, S. S.; Lee, S.; Oh, H. B. Noncovalent complexes of cyclodextrin with small organic molecules: Applications and insights into

host–guest interactions in the gas phase and condensed phase. *Molecules* **2020**, *25*, 4048. https://doi.org/10.3390/molecules25184048

36. Amran, F.; Zaini, M.A.A. Beta-cyclodextrin adsorbents to remove water pollutants – a commentary. *Front. Chem. Sci. Eng.* **2022**, *16*, 1 – 17. https://doi.org/10.1007/s11705-022-2146-2

37. Ariff M.M.; Zaini M.A.A. Carbon-based beta-cyclodextrin adsorbent for methylene blue and reactive orange 16 removal from water. *Acta Chem. Iasi* **2020**, *28*, 19 – 30. https://doi.org/10.2478/achi-2020-0002

38. Wang, Y.; Zhou, A. Spectroscopic studies on the binding of methylene blue with DNA by means of cyclodextrin supramolecular systems. *J. Photochem. Photobiol. A* **2007**, *190*, 121 – 127. https://doi.org/10.1016/j.jphotochem.2007.03.020